*Journal of Engineering, Emerging Technologies and Applied Sciences*
*Volume: 03 Issue: 01 | March, 2026* Access point: ***https://www.ndu.edu.ng/jeetas***

# Liquid Phase Direct Chlorination of Ethylene for the Production of Ethylene Dichloride in a Mixed Flow Reactor

Chimene O. Wosu[1], Precious P. George[2], Lesi N. Nwiabu [3]

[1]*Department of Chemical Engineering, Federal University Otuoke, Bayelsa State, Nigeria*
Email: wosuco@fuotuoke.edu.ng

[2]*Department of Chemical/Petrochemical Engineering, Rivers State University, Rivers State, Nigeria*

[3]*Department of Chemical Engineering, Federal University Otuoke, Bayelsa State, Nigeria*

## ABSTRACT

*This research considered the design of a Mixed Flow Reactor (MFR) using MATLAB simulation design for the production of 1,000,000 tons (1,000,000,000 kg) per year of ethylene dichloride from the liquid-phase direct chlorination of ethylene. The study employed fundamental design equations and MATLAB simulations to evaluate key operating parameters including volume, height, diameter, space time, space velocity, quantity of heat generated and the quantity of heat generated per unit volume of the reactor at 95% fractional conversion were gotten as 0.069m3, 0.7063m, 0.3532m, 0.01162seconds, 86.05seconds, 8.44 × 107 J/s and 1.22× 109 J/sm3 respectively. Results revealed that chlorine is the limiting reactant, while ethylene remains in excess, permitting a pseudo-first-order kinetic treatment. Conversion was found to increase with higher temperature, residence time, and reactor size, but declined at elevated space velocities. The highly exothermic nature of the process highlighted the need for effective heat management to ensure safe and stable operation. The evaluation of the MFR yearly production dependent on the reactor volume stood at $ 112,573. Overall, the design demonstrated that an optimised operating temperature of 357 K, coupled with adequate reactor sizing and efficient cooling, can achieve high conversion and economic production of EDC, providing a reliable framework for industrial application.*

***Keywords — Ethylene, Chlorination, Mixed Flow Reactor, Design, Ethylene Dichloride.***

## 1. INTRODUCTION

Ethylene dichloride (EDC) is a chlorinated hydrocarbon and one of the most vital intermediates utilized in chemical industries globally, primarily serves as a precursor for the production of polyvinyl chloride, methyl chloroform, trichloroethylene, perchloroethylene, vinylidene chloride, ethylene amines and other useful intermediates for the production of plastics, corrosion inhibitors, pesticides, lead scavenger in gasoline, degreasing, cleaning and dry-cleaning processes. Industrially, ethylene dichloride production is via liquid-phase direct chlorination if ethylene in a mixed flow reactor (MFR) in the presence of iron III chloride ($FeCl_3$) as a catalyst. The $FeCl_3$ catalyst is preferred due to its characteristics of promoting the formation of EDC while inhibiting the formation of unwanted by-products. Also, $FeCl_3$ is capable of lowering the activation energy, thus improving the reaction kinetics of the process (Kurta

  

*et al*., 2018). The reaction vessel (MFR) is widely adopted due to its operational principles such as uniform mixing, advanced heat management for exothermic nature of chlorination, mitigation of risks associated with thermal runaway as well as improving energy efficiency (Wang & Ma, 2022; Wosu & Aworabhi, 2025a; Wosu & Aworabhi, 2025b).

The research however considered the design of a MFR for catalytic liquid-phase chlorination of ethylene for ethylene dichloride production. The reactor design was performed from the application of the conservation principles of mass and energy for the development of models for reactor parameters such as volume, height, diameter, space time, space velocity, quantity of heat generated as well as the quantity of heat generated per unit volume of the reactor which was solved using MATLAB R2023a. This research becomes highly imperative for effective and efficient production of ethylene dichloride as well as the sustainability of the petrochemical product.

## 2. LITERATURE REVIEW

Ethylene dichloride (EDC), also known as 1,2-dichloroethane, is an important chlorinated hydrocarbon primarily produced for the manufacture of vinyl chloride monomer (VCM), which serves as the principal precursor for polyvinyl chloride (PVC). The large global demand for PVC in construction materials, piping systems, packaging, and chemical intermediates has sustained the industrial importance of EDC production processes. Commercial manufacturing routes for EDC include direct chlorination of ethylene, oxychlorination of ethylene, and integrated processes combining both reactions to optimize chlorine utilization. Among these routes, liquid-phase direct chlorination of ethylene remains one of the most widely applied industrial methods because of its high selectivity, relatively simple reaction pathway, and efficient conversion of reactants under controlled conditions (Benvenuto & Plaumann, 2021; Intratec, 2022).

In the liquid-phase direct chlorination process, gaseous ethylene and chlorine react in the presence of a liquid ethylene dichloride medium, which serves simultaneously as solvent and reaction environment. Catalytic additives such as ferric chloride are commonly introduced to accelerate the chlorination reaction and improve reaction stability. Experimental investigations of the reaction mechanism indicate that chlorination proceeds through a radical chain mechanism initiated by the homolytic dissociation of chlorine molecules, forming chlorine radicals that subsequently react with ethylene to produce chlorinated intermediates before yielding ethylene dichloride as the final product (Kurta *et al*., 2018). Kinetic studies reported in experimental reactor investigations have shown that the reaction rate exhibits approximately first-order dependence on both ethylene and chlorine concentrations, indicating that increases in the concentration of either reactant directly influence the rate of ethylene dichloride formation (Wachi & Morikawa, 1986).

The thermodynamic behavior of the direct chlorination reaction plays a crucial role in reactor design because the reaction is strongly exothermic. Reported heat of reaction values range between −218 and −230 kJ per mole of ethylene dichloride produced, indicating substantial heat release during operation. This high heat generation requires effective temperature control strategies in industrial reactors in order to prevent thermal runaway and maintain product selectivity (Intratec, 2022). Industrial chlorination units therefore incorporate heat removal systems such as external cooling jackets, internal cooling coils, and circulating heat exchange loops designed to maintain stable reactor temperatures during continuous operation. Reported overall heat transfer coefficients for these cooling systems typically fall within the range of 300 to 900 $W/m^2K$ depending on reactor configuration and heat removal method (Moradi & Farsi, 2020).

Industrial liquid-phase chlorination reactors generally operate as gas–liquid systems in which

  

gaseous ethylene and chlorine are dispersed into a liquid ethylene dichloride phase through spargers or injection nozzles. In such systems, both intrinsic chemical kinetics and gas–liquid mass transfer influence the overall reaction rate. Modelling studies of industrial chlorination reactors have shown that gas-liquid mass transfer parameters significantly affect the absorption of chlorine into the liquid phase and therefore influence reaction efficiency. Typical volumetric gas–liquid mass transfer coefficients reported for such systems range between 0.02 and 0.5 $s^{-1}$ depending on mixing intensity and reactor hydrodynamics (Moradi & Farsi, 2020).

Several reactor configurations have been investigated for ethylene chlorination processes, including bubble column reactors, external loop gas-lift reactors, and mechanically agitated continuous stirred tank reactors. Industrial studies of bubble column chlorination reactors have demonstrated that external recirculation loops improve mixing, enhance heat removal, and increase gas dispersion within the liquid reaction medium. In one industrial reactor model, a reactor volume of approximately 19 $m^3$ was reported to achieve an annual ethylene dichloride production capacity of about 54,000 tons under optimized conditions (Orejas, 2001). External-loop gas-lift reactors have also been examined for this process due to their ability to promote natural liquid circulation between riser and downcomer sections, thereby improving gas dispersion and hydrodynamic stability within the reactor system (Abashar, 2004).

Continuous stirred tank reactors, also referred to as mixed flow reactors, are particularly suitable for highly exothermic liquid-phase reactions because they provide excellent mixing and uniform temperature distribution throughout the reactor volume. Efficient mixing ensures that concentration and temperature gradients are minimized, thereby improving process stability and reducing the formation of undesired by-products. Studies on reactor mixing behavior have shown that continuous stirred tank reactors allow rapid dispersion of gaseous reactants in liquid media, making them suitable for reactions involving gas-liquid interactions and high heat release (Cherkasov *et al*., 2022).

Industrial operating conditions for liquid-phase ethylene chlorination are typically maintained within moderate temperature and pressure ranges in order to optimize conversion and maintain liquid phase conditions. Reported operating temperatures commonly fall between 45 and 70 °C, while reactor pressures are generally maintained between 2 and 5 bar to improve ethylene solubility in the liquid phase and enhance reaction efficiency (Intratec, 2022; Orejas, 2001). Ethylene is frequently supplied in slight excess relative to chlorine to suppress the formation of higher chlorinated by-products such as trichloroethane and tetrachloroethane, thereby improving selectivity toward ethylene dichloride (EPA, 1984). Under well-controlled industrial conditions, ethylene conversion values between 90 and 98 percent and product selectivity greater than 95 percent have been reported for direct chlorination processes.

Advances in reactor modelling and computational simulation have further improved understanding of ethylene chlorination processes. Integrated models combining chemical kinetics, hydrodynamic behavior, and mass transfer phenomena have been used to evaluate reactor performance and optimize industrial operating conditions. Such modelling approaches allow engineers to predict reactor behavior under different operating scenarios and provide valuable guidance for the design and scale-up of mixed flow reactors used in ethylene dichloride production (Moradi & Farsi, 2020).

## 3. MATERIALS AND METHODS

The required materials for this research are a laptop, journals, textbooks and the simulation tool used is MATLAB.

  

Journal of Engineering, Emerging Technologies and Applied Sciences
Volume: 03 Issue: 01 | March, 2026 Access point: https://www.ndu.edu.ng/jeetas

This research employs a quantitative methodology, utilizing data acquired from the thermodynamic parameters of reactant species and products, as well as literature, plant data, and computed or derived information. The procedures utilized in this research are;

i. Development of the reaction kinetic models
ii. Development of design or sizing models for reactor volume, height, diameter, space time, space velocity, quantity heat generated, and heat generated per unit volume of the reactor.
iii. Energy balance model development

### 3.1. Development of the Reaction Kinetic Models

The kinetic models for liquid phase direct chlorination of ethylene for ethylene dichloride production, can be derived from the reaction kinetics of the process.

$$CH_4 + Cl_2 \xrightarrow{k_1} C_2H_4Cl_2 \quad (1)$$

Equation (1) can be expressed symbolically as

$$A + B \xrightarrow{k_1} C \quad (2)$$

where A and B are reactant species (Ethylene and Chlorine), C represents the product (ethylene dichloride) and $k_1$ is the kinetic rate constant which is an indication that the reaction process is temperature dependent and the process condition is non-isothermal. The rate law of the liquid-phase direct chlorination reaction can be expressed as a function of feed rate depletion as:

$$-r_A = \frac{-dC_A}{dt} = k_1 C_A C_B \quad (3)$$

Where $C_A = C_{Ao}(1 - x_A)$ (4)

$$C_B = C_{Bo} - C_{Ao}x_A \text{ or } C_B = C_{Ao}(m - x_A) \quad (5)$$

$$\therefore -r_A = k_1 {C_{Ao}}^2 (1 - x_A)(m - x_A) \quad (6)$$

where $-r_A$ is the rate of depletion of the limiting reactant specie, $C_{Ao}$ is the initial concentration of reactant species A and B in mol/m$^3$, $k_1$ is the rate constant $m$ is the ratio of excess and limiting reactant, $m = \frac{C_{Bo}}{C_{Ao}}$, and $x_A$ is the fractional conversion of specie $A$.

### 3.2. Development of MFR Design/Sizing Models

Consider the schematic representation of a mixed flow reactor with feed and product streams.

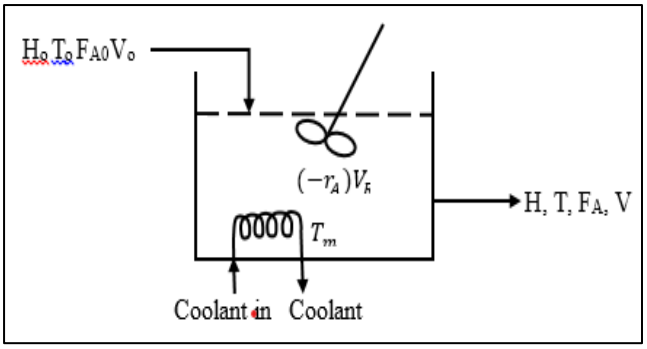


*Figure 1: A Typical Mixed Flow Reactor*

The MFR design models can be developed by performing mass and energy balance over the reactor with the following assumptions.

i. The feed assumes a uniform composition throughout the reactor.
ii. The reacting mixture is well stirred
iii. The composition of the exit stream is the same as that within the reactor.
iv. Shaft work by the impeller or stirrer is negligible.
v. The temperature within the reactor is kept at a constant value by the heat exchange medium.

  

Journal of Engineering, Emerging Technologies and Applied Sciences
Volume: 03 Issue: 01 | March, 2026 Access point: https://www.ndu.edu.ng/jeetas

### 3.2.1. Volume of the Reactor Determination ($V_R$)

This can be obtained by applying the principle of material balance stated as follows:

$$\begin{bmatrix}\text{Rate of accumulation of material within the volume}\end{bmatrix} = \begin{bmatrix}\text{Rate of input of feed into the volume}\end{bmatrix} - \begin{bmatrix}\text{Rate of outflow of feed from the volume}\end{bmatrix} - \begin{bmatrix}\text{Rate of depletion of feed due to chemical reaction}\end{bmatrix} \quad (7)$$

$$\begin{bmatrix}\text{Rate of accumulation of material within the volume}\end{bmatrix} = \frac{d}{dt}(C_A V_R) \quad (8)$$

$$\begin{bmatrix}\text{Rate of input of feed to the volume}\end{bmatrix} = F_{Ao} \quad (9)$$

$$\begin{bmatrix}\text{Rate of output of feed from the volume}\end{bmatrix} = F = F_{Ao}(1 - x_A) \quad (10)$$

$$\begin{bmatrix}\text{Rate of depletion of feed due to chemical reaction}\end{bmatrix} = (-r_A)V_R \quad (11)$$

The terms from equation (8) to (11) can be defined, substituted and simplified into (7) to give;

$$\frac{d}{dt}(C_A V_R) = F_{Ao} - [F_{Ao}(1 - x_A)] - (-r_A)V_R \quad (12)$$

At steady state, the accumulation term is equal to zero, i.e.:

$$\frac{d}{dt}(C_A V_R) = 0$$

Therefore;

$$0 = F_{Ao} - [F_{Ao}(1 - x_A)] - (-r_A)V_R \quad (13)$$

Expanding the bracket:

$$0 = F_{Ao}x_A - (-r_A)V_R$$

$$V_R = \frac{F_{Ao}x_A}{(-r_A)} \quad (14)$$

Substituting equation (6) into (10) yields;

$$V_R = \frac{F_{Ao}x_a}{k_o {C_{Ao}}^2 e^{-E/RT}(1-x_A)(m-x_A)} \quad (15)$$

Where equation (15) is the reactor volume ($V_R$). The height of the reactor ($H_R$) is given as:

$$H_R = \left(\frac{16V_R}{\pi}\right)^{\frac{1}{3}} \quad (16)$$

$$\therefore H_R = \left[\frac{16F_{Ao}x_A}{\pi k_o {C_{Ao}}^2 e^{-E/RT}(1-x_A)(m-x_A)}\right]^{\frac{1}{3}} \quad (17)$$

For Diameter of the reactor ($D_R$),

$$D_R = \frac{H_R}{2} \quad (18)$$

$$\therefore D_R = \frac{\left[\frac{16F_{Ao}x_A}{\pi k_o {C_{Ao}}^2 e^{-E/RT}(1-x_A)(m-x_A)}\right]^{\frac{1}{3}}}{2} \quad (19)$$

Space time of the reactor ($\tau_{MFR}$) is given as;

$$\tau_{MFR} = \frac{V_R}{V_o} \quad (20)$$

$$\tau_{MFR} = \frac{\frac{F_{Ao}x_A}{k_o {C_{Ao}}^2 e^{-E/RT}(1-x_A)(m-x_A)}}{V_o} \quad (21)$$

But; $F_{Ao} = C_{Ao}v_o$ (22)

$$\therefore \tau_{MFR} = \frac{x_A}{k_o {C_{Ao}}^2 e^{-E/RT}(1-x_A)(m-x_A)} \quad (23)$$

and Space velocity ($S_V$) is given as;

$$S_V = \frac{1}{\tau_{MFR}} \quad (24)$$

$$\therefore S_V = \frac{k_o C_{Ao}\ e^{-E/RT}(1-x_A)(m-x_A)}{x_A} \quad (25)$$

### 3.2.2. Quantity of Heat Determination (Q)

The quantity of heat generated and the quantity of heat generated per unit volume of the reactor are expressed mathematically as:

  

Journal of Engineering, Emerging Technologies and Applied Sciences
Volume: 03 Issue: 01 | March, 2026 Access point: https://www.ndu.edu.ng/jeetas

$$Q = \Delta H_R F_{Ao} x_A \quad (26)$$

$$q = \frac{Q}{V_R}$$

$$q = \frac{\Delta H_R F_{Ao} x_A}{V_R} \quad (27)$$

where $Q$ is the quantity of heat $(J/K)$, $q$ is the quantity of heat generated per unit volume of the reactor, $\Delta H_R$ is the heat of reaction $(kJ/mol)$, $F_{Ao}$ is the flow rate of reactant species (mol/s) and $x_A$ is the fractional conversion of species (dimensionless)

### 3.3. Energy Balance Model Development

Performing an energy balance over the reactor yields;

$$\begin{bmatrix}\text{Rate of accumulation of heat within the volume}\end{bmatrix} = \begin{bmatrix}\text{Rate of Input of heat to the volume}\end{bmatrix} - \begin{bmatrix}\text{Rate of Output of heat from the volume}\end{bmatrix} - \begin{bmatrix}\text{Rate of depletion of heat due to chemical reaction}\end{bmatrix} - \begin{bmatrix}\text{Rate of heat removal to the surrounding}\end{bmatrix} + \begin{bmatrix}\text{Shaft work done by the shirrer}\end{bmatrix} \quad (28)$$

$$\begin{bmatrix}\text{Rate of accumulation of heat within the volume}\end{bmatrix} = \frac{d(\rho V c_p T)}{dt} \quad (29)$$

$$\begin{bmatrix}\text{Rate of Input of heat to the volume}\end{bmatrix} = \rho v_o c_p T_o \quad (30)$$

$$\begin{bmatrix}\text{Rate of outflow of heat from the volume}\end{bmatrix} = \rho V c_p T \quad (31)$$

$$\begin{bmatrix}\text{Rate of depletion of heat due to chemical reaction}\end{bmatrix} = (-r_A)V_R(\Delta H_R) \quad (32)$$

$$\begin{bmatrix}\text{Rate of heat removal to the surrounding}\end{bmatrix} = UA_c(T - T_c) \quad (33)$$

$$\begin{bmatrix}\text{Shaft work done by the shirrer}\end{bmatrix} = w_s \quad (34)$$

The terms from equation (8) to (11) can be defined, substituted and simplified into (7) to give the energy balance model as;

$$\rho v_o c_p \frac{dT}{dt} = \rho v_o c_p T_o - \rho v_o c_p T - (-r_A)V_R(\Delta H_R) - UA_c(T - T_c) = W_s \quad (35)$$

At steady state,

$$\frac{dH}{dt} = \rho c_p v \frac{dT}{dt} = 0$$

Also neglecting the shaft work, $w_s$, equation (35) becomes

$$0 = \rho v_o c_p T_o - \rho v_o c_p T - (-r_A)V_R(\Delta H_R) - UA_c(T - T_c)$$

$$\rho v_o c_p (T - T_o) = -(r_A)V_R(\Delta H_R) - UA_c(T - T_c)$$

$$T - T_o = \frac{(-r_A)V_R(\Delta H_R)}{\rho v_o c_p} - \frac{UA_c(T - T_c)}{\rho v_o c_p} \quad (36)$$

But $\frac{V_R}{V_o} = \tau$ (Space time)

$$T - T_o = \tau\frac{(-r_A)(\Delta H_R)}{\rho c_p} - \frac{UA_c(T - T_c)}{\rho v_o c_p} \quad (37)$$

$$\therefore T = \frac{\tau \Delta H_R r_A v_o + UA_c T_c + \rho v_o c_p T_o}{\rho v_o C_p + UA_c} \quad (38)$$

The capital cost for yearly production of ethylene dichloride as a function of the MFR volume at

  

maximum fractional conversion is given by (John, 2007).

$$\text{Cost} = \$200{,}000 \left(\frac{V_{MFR}}{1000}\right)^{0.6} \quad (30)$$

where $V_{MFR}$ is the volume of MFR in $m^3$. The above model is for a life of 20years with no salvage values.

### 3.3.1. Solution Techniques

The design for functional parameters of the reactor and temperature effect models can be solved using advanced process simulation software (MATLAB). The Algorithm for the simulation process is shown in Figure 2.

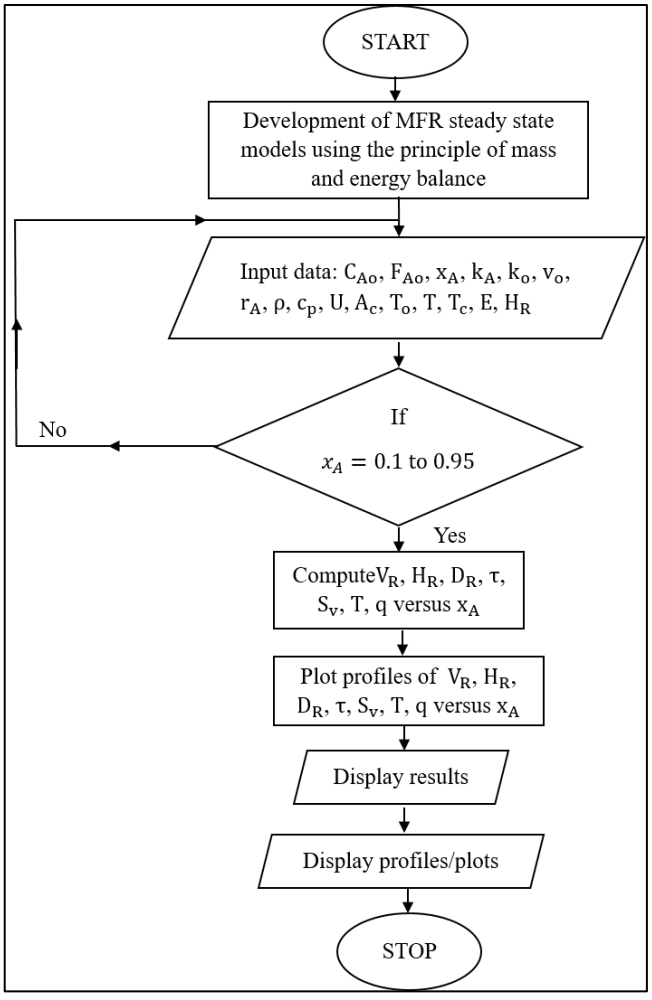


*Figure 2: Algorithm of the Simulation Process*

### 3.3.2. Data for Evaluation

The data for evaluation in this research are the properties/thermodynamic data, calculated/derived data and data obtained from literatures as presented in table 1, 2 and 3 respectively.

*Table 1: Properties/Thermodynamic Data*

| Data/ Parameter | Values | Description |
|---|---|---|
| $\rho_A$ | 560Kg/$m^3$ | Density of ethylene |
| $\rho_B$ | 2.89Kg/$m^3$ | Density of chlorine |
| $\rho_C$ | 1,253Kg/$m^3$ | Density of ethylene dichloride |
| R | 8.314 $Nmmol^{-1}K^{-1}$ | Gas Constant |

*Table 2: Data Obtained from Literature*

| Data | Values | Description | References |
|---|---|---|---|
| $T_o$ | 287.8K | Initial temperature of feed | Wachi & Morikawa, 1986 |
| T | 357K | Operating temperature | Moradi & Farsi, 2020 |
| $T_c$ | 318K | Coolant temperature | Junsittiwate *et al.*, 2018 |
| $k_1$ | 0.132$m^3$ $mol^{-1}s^{-1}$ | Rate constant | Wachi & Morikawa, 1986 |
| E | 20.1KJ/mol | Activation energy | Wachi & Morikawa, 1986 |
| - ΔHr | -218 KJ/mol | Heat of reaction | Moradi & Farsi, 2020 |

  

*Table 3: Calculated Design Data*

| Data/Parameter | Values | Description |
|---|---|---|
| $M_A$ | 0.028Kg/mol | Molecular weight of ethylene |
| $M_B$ | 0.071Kg/mol | Molecular weight of chlorine |
| $M_C$ | 0.099Kg/mol | Molecular weight of ethylene dichloride |
| $\dot{m}_A$ | 10.9116Kg/s | Mass flow rate of ethylene |
| $\dot{m}_B$ | 27.6687Kg/s | Mass flow rate of chlorine |
| $\dot{m}_C$ | 38.5803Kg/s | Mass flow rate of ethylene dichloride |
| $\bar{V}_A$ | 0.0018$m^3$/kg | Specific density of ethylene |
| $\bar{V}_B$ | 0.346$m^3$/kg | Specific density of chlorine |
| $\bar{V}_C$ | 0.0008$m^3$/kg | Specific density of ethylene dichloride |
| $Q_A$ | 0.0196$m^3$/s | Volumetric flow rate of ethylene |
| $Q_B$ | 9.5734$m^3$/s | Volumetric flow rate of chlorine |
| $v_o$ | 5.953$m^3$/s | Total volumetric flow rate of reactants |
| $C_{Ao}$ | 42.46mol/$m^3$ | Initial concentration of limiting reactant |
| $C_{Bo}$ | 20,000mol/$m^3$ | Initial concentration of liquid ethylene |
| $m$ | 471.0316 | ratio of excess and the limiting reactant |
| $F_{Ao}$ | 407.3188mol/s | Initial molar flow rate of limiting reactant |
| $X_A$ | 0.95 (Dimensionless) | Maximum fractional conversion |

## 4. RESULTS AND DISCUSSION

### 4.1. Design Results

This chapter presents the results obtained from the MATLAB simulation of a Mixed Flow Reactor (MFR) design for the production of 1,000,000 tons (1,000,000,000 kg) per year of ethylene dichloride from the liquid-phase direct chlorination of ethylene at 95% fraction conversion. The simulation results are shown in the tabular form in Table 4.

*Table 4: MATLAB Simulation Results Showing Fractional Conversion, Temperature, Reactor Volume, Height, Diameter, Space Time, Space Velocity, Quantity of Heat Generated and Quantity of Heat Generated per Unit Volume of the Reactor is Presented.*

| $X_A$ | T(K) | $V_R$ ($m^3$) | $H_R$ (m) | $D_R$ (m) | τ(s) | $S_V$ ($s^{-1}$) | Q (J/s) | q (J/$m^3$s) |
|---|---|---|---|---|---|---|---|---|
| 0.00 | 357 | 0.0000 | 0.0000 | 0.0000 | 0.0000 | Inf | 0.0000 | NaN |
| 0.05 | 357 | 0.0002 | 0.0991 | 0.0496 | 3.213E-05 | 31124 | 4439800 | 2.3212E10 |
| 0.10 | 357 | 0.0004 | 0.1272 | 0.0636 | 6.7837E-05 | 14741 | 8879500 | 2.1988E10 |
| 0.15 | 357 | 0.0006 | 0.1484 | 0.0742 | 0.000108 | 9280.6 | 13319000 | 2.0765E10 |
| 0.20 | 357 | 0.0009 | 0.1666 | 0.0833 | 0.000153 | 6550.3 | 17759000 | 1.9541E10 |
| 0.25 | 357 | 0.0012 | 0.1834 | 0.0917 | 0.000204 | 4912.2 | 22199000 | 1.8318E10 |
| 0.30 | 357 | 0.0016 | 0.1995 | 0.0997 | 0.000262 | 3820.2 | 26639000 | 1.7095E10 |
| 0.35 | 357 | 0.0020 | 0.2152 | 0.1076 | 0.000329 | 3040.2 | 31078000 | 1.5872E10 |

  

Journal of Engineering, Emerging Technologies and Applied Sciences
Volume: 03 Issue: 01 | March, 2026 Access point: https://www.ndu.edu.ng/jeetas

| $X_A$ | T(K) | $V_R$ ($m^3$) | $H_R$ (m) | $D_R$ (m) | τ(s) | $S_V$ ($s^{-1}$) | Q (J/s) | q ($J/m^3s$) |
|---|---|---|---|---|---|---|---|---|
| 0.40 | 357 | 0.0024 | 0.2311 | 0.1156 | 0.000407 | 2455.3 | 35518000 | 1.465E10 |
| 0.45 | 357 | 0.0030 | 0.2475 | 0.1237 | 0.000499 | 2000.4 | 39958000 | 1.3427E10 |
| 0.50 | 357 | 0.0036 | 0.2646 | 0.1323 | 0.000611 | 1636.5 | 44398000 | 1.2205E10 |
| 0.55 | 357 | 0.0045 | 0.2829 | 0.1415 | 0.000747 | 1338.8 | 48838000 | 1.0984E10 |
| 0.60 | 357 | 0.0055 | 0.3029 | 0.1515 | 0.000917 | 1090.8 | 53277000 | 9.7622E09 |
| 0.65 | 357 | 0.0068 | 0.3253 | 0.1626 | 0.001135 | 880.93 | 57717000 | 8.541E09 |
| 0.70 | 357 | 0.0085 | 0.351 | 0.1755 | 0.001426 | 701.07 | 62157000 | 7.32E09 |
| 0.75 | 357 | 0.0109 | 0.3817 | 0.1908 | 0.001834 | 545.22 | 66597000 | 6.0994E09 |
| 0.80 | 357 | 0.0146 | 0.4201 | 0.2101 | 0.002446 | 408.87 | 71036000 | 4.879E09 |
| 0.85 | 357 | 0.0206 | 0.4719 | 0.2359 | 0.003465 | 288.58 | 75476000 | 3.6589E09 |
| 0.90 | 357 | 0.0327 | 0.5506 | 0.2753 | 0.005504 | 181.68 | 79916000 | 2.439E09 |
| 0.95 | 357 | 0.0692 | 0.7063 | 0.3532 | 0.011621 | 86.051 | 84356000 | 1.2194E09 |

Table 4 shows the MATLAB simulation results of the MFR at varying fractional conversion. From the table, the reactor parameters such volume, height, diameter, space time and quantity of heat generated increases as the fractional conversion increases which clearly shows that the more the feed materials are used up or converted, the more the yield of the target product (ethylene dichloride). Also, a decrease in space velocity and quantity of heat generated per unit volume of the reactor was observed as the fractional conversion increases, this behaviour validates the mathematical expression of the reactor parameters (Wosu & Aworabhi, 2025a). At maximum conversion of 0.95, the reactor volume, height, diameter, space time, space velocity, quantity of heat generated as well as quantity of heat generated per unit volume of the reactor stood at $0.069m^3$, $0.7063m$, $0.3532m$, $0.01162seconds$, $86.05seconds$, $8.44 \times 10^7$ J/s and $1.22\times 10^9$ $J/sm^3$ respectively.

#### *4.1.1. Variation of Temperature with Fractional Conversion*

Figure 3 below shows a graph of fractional conversion ($X_A$) and reactor temperature (T) which showed the graphical relationship between the operating temperature and fractional conversion.

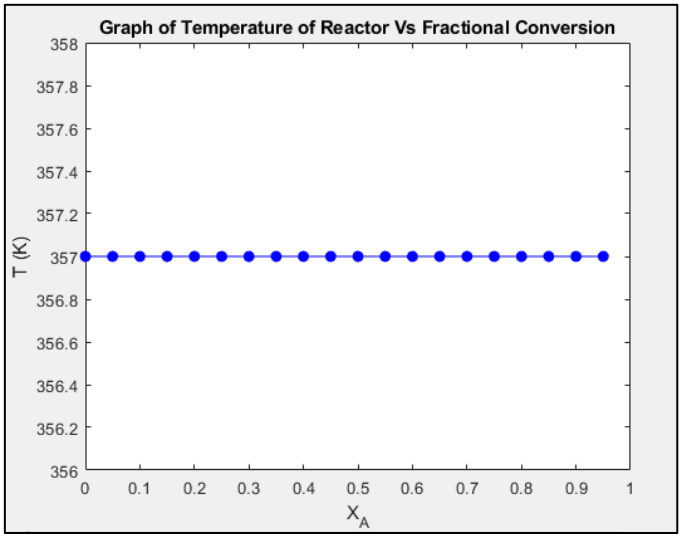


***Figure 3: Profile of Temperature (T) with Fractional Conversion ($X_A$)***

  

According to the profile, the operating temperature of 357K remains constant even at varying fractional conversion during the EDC production process from the direct chlorination of ethylene and chlorine. At operating temperature well below or well above the limit of specification for EDC production will result to poor performance of the reactor or low productivity of the process. (Moradi & Farsi, 2020).

### *4.1.2. Variation of Reactor Volume with Fractional Conversion*

It can be seen from the plot between fractional conversion XA and reactor volume (VR) in figure 4 exhibited an exponential growth pattern.

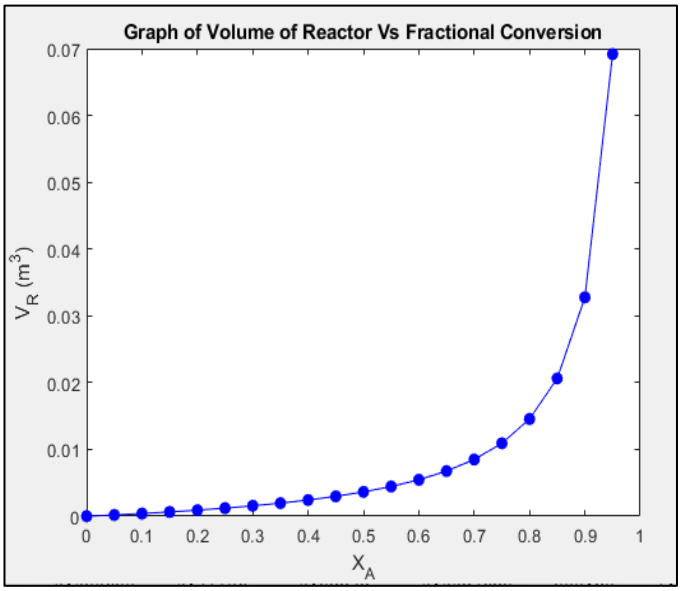


***Figure 4: Profile of Reactor Volume ($V_R$) with Fractional Conversion ($X_A$)***

At low conversion (XA = 0.05), the reactor volume was very minimal, about 0.0002$m^3$, indicating minimal residence time. As conversion increased to XA= 0.5, the volume rose moderately to around 0.0036$m^3$, suggesting more reactor space was needed to sustain the reaction. However, a rapid increase occurred beyond XA = 0.8, where the reactor volume expanded sharply to about 0.692$m^3$ at XA = 0.95. The pronounced curvature at higher conversion reflects the declining rate of reaction as reactant concentration decreases, thus requiring larger volumes for further conversion. The close clustering of points at low conversion indicates faster reaction kinetics in the early stages, while the spreading at high conversion marks the region where reactor design must compensate for slower kinetics through volume expansion (Kurta et al. 2018).

### *4.1.3. Variation of Reactor Volume with Fractional Conversion*

The variation of fractional conversion with reactor height displayed a nearly linear yet slightly exponential rise as shown in figure 5. At $X_A = 0.05$, the height was approximately $0.09\text{m}$, increasing to about $0.26\text{m}$ at $X_A = 0.5$, and reaching a maximum of approximately $0.7\text{m}$ at $X_A = 0.95$.

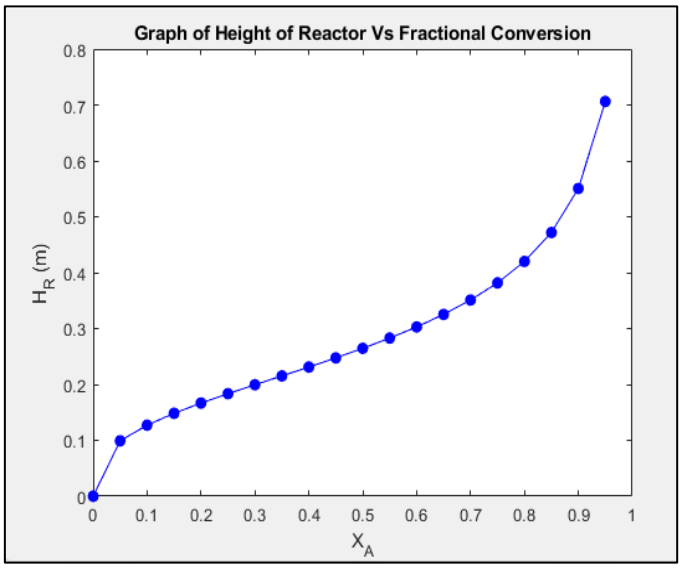


***Figure 5: Profile of Reactor Height ($H_R$) with Fractional Conversion ($X_A$)***

The graph shows a steady slope from low to medium conversion, after which the rise becomes more pronounced. This indicates that as conversion increases, a proportionally greater reactor height is required to maintain the necessary residence volume. The curve's inflection beyond $X_A = 0.8$ marks

  

the region of diminishing return where additional reactor height yields smaller improvements in conversion. The close spacing of points between $X_A$ = 0.05 and 0.5 shows a gradual change, while the wide spacing toward $X_A$ = 0.95 reflects a sharp volumetric expansion due to reduced reaction rate at high conversion.

#### *4.1.4. Variation of Reactor Diameter with Fractional Conversion*

The plot of fractional conversion against reactor diameter showed a gentle upward curve, signifying that diameter increases progressively with conversion (figure 6).

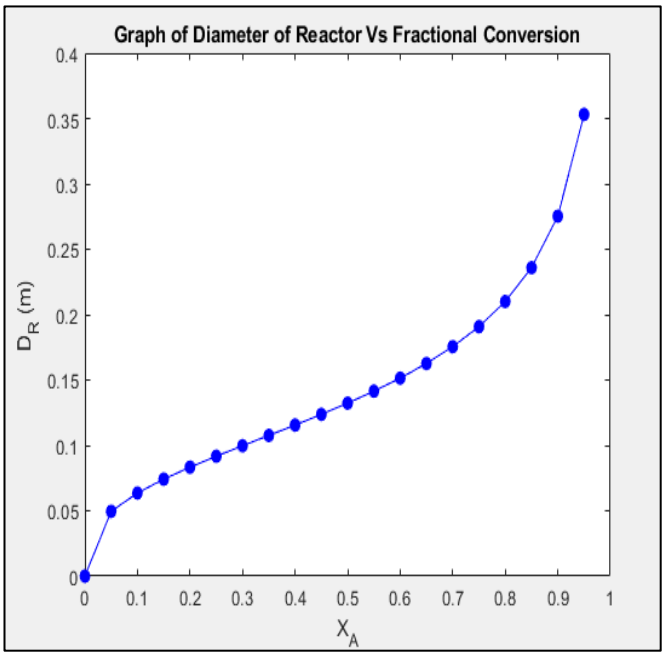


***Figure 6: Profile of Reactor Diameter (DR) with Fractional Conversion ($X_A$)***

At low conversion ($X_A$ = 0.05), the diameter was approximately 0.05m, indicating a compact reactor section. As conversion rose to $X_A$ = 0.5, the diameter increased gradually to about 0.13m, while at higher conversion near $X_A$ = 0.95, it reached about 0.35m. The smooth and slightly curved pattern of the graph shows that reactor expansion in diameter is moderate across most of the conversion range. The closer spacing of data points between $X_A$ = 0.05 and 0.8 suggests a stable rate of volumetric increase, whereas wider spacing beyond $X_A$ = 0.85 reflects accelerated radial expansion. This behaviour highlights that while reactor height governs residence volume more significantly, diameter adjustments play an important role in improving mixing efficiency at higher conversions (Wosu & Aworabhi, 2025a).

#### *4.1.5. Variation of Space-Time with Fractional Conversion*

The curve representing space-time as a function of fractional conversion in figure 7 exhibits an exponential increase.

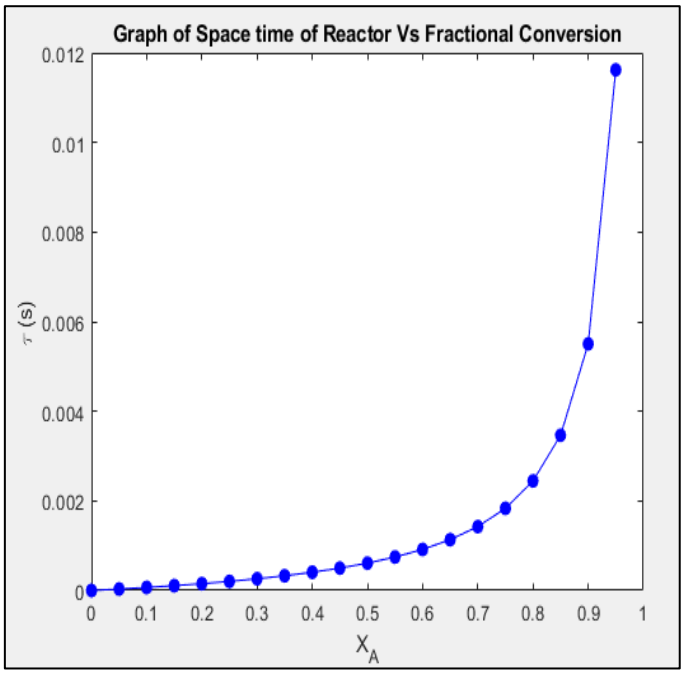


***Figure 7: Profile of Space Time (τ) with Fractional Conversion ($X_A$)***

At low conversion ($X_A$ = 0.05), the space time was only about $3.2\times10^{-5}$ s, showing that minimal residence time was required when the reaction rate was high. At a mid-range conversion ($X_A$ = 0.5), the

  

space time increased sharply to approximately $6.1\times10^{-4}$ s, while at high conversion ($X_A = 0.95$), it rose dramatically to about 0.01s. The curvature indicates that achieving higher conversion requires much longer residence time due to decreasing reactant concentration and slower reaction rate. The compact clustering of data points below $X_A = 0.6$ shows that the reaction proceeds quickly at the initial stage, while the steep rise and wider spacing beyond $X_A = 0.8$ emphasize that further conversion becomes increasingly difficult and time-dependent.

#### *4.1.6. Variation of Space Velocity with Fractional Conversion*

The relationship between space velocity and fractional conversion displayed a steep negative slope, confirming the inverse dependence between $S_V$ and τ.

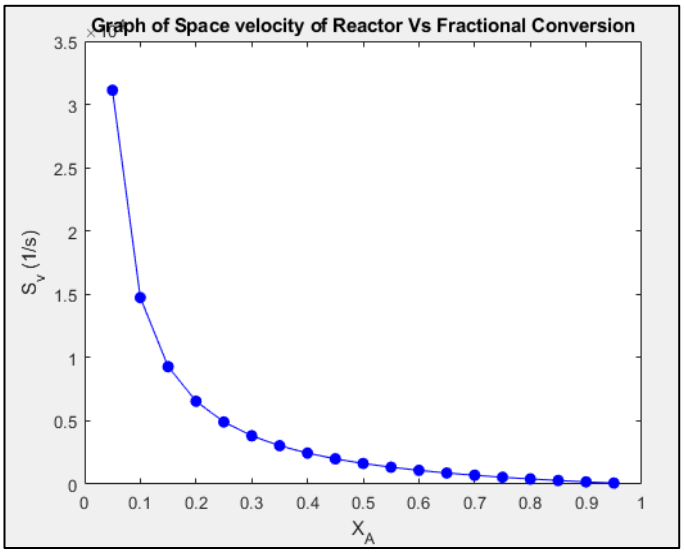


***Figure 8: Profile of Space Velocity ($S_V$) with Fractional Conversion ($X_A$)***

At $X_A = 0.05$, space velocity was about $3.1\times10^4$ $s^{-1}$, signifying a high feed turnover rate at low conversion. As conversion reached $X_A = 0.5$, space velocity decreased drastically to around 1,636 $s^{-1}$, and further dropped to approximately 86 $s^{-1}$ at $X_A = 0.95$. The curve shows a sharp decline up to $X_A = 0.6$ and then gradually flattens, indicating that as conversion progresses, feed throughput per unit reactor volume must decrease to sustain reaction completion. The compacted points at lower conversion demonstrate rapid feed cycling, while the sparse spacing at higher conversion highlights the need for extended residence time to achieve higher yields.

#### *4.1.7. Variation of Heat Generated with Fractional Conversion*

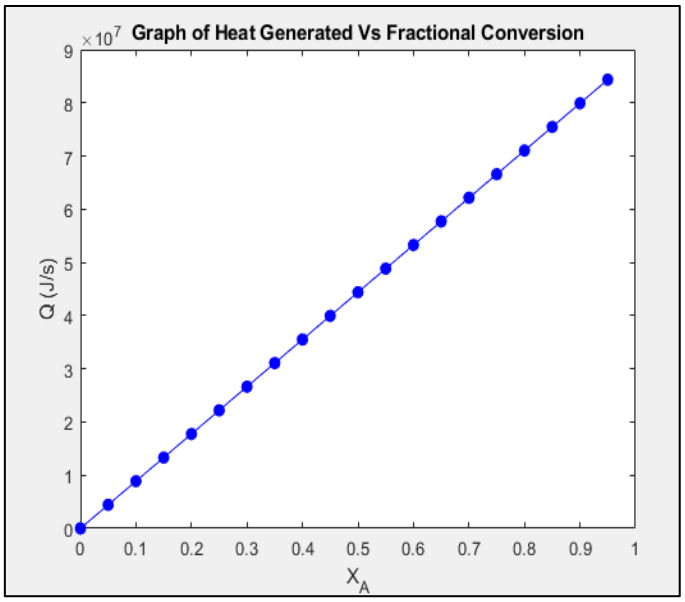


***Figure 9: Profile of Heat Generated (Q) with Fractional Conversion ($X_A$)***

The direct relation of heat generated against conversion followed a rising exponential trend. From low conversion ($X_A = 0.05$), Q was about $4.4\times10^6$ J/s, while rising linearly through mid-point ($X_A = 0.5$) at approximately $4.4\times10^7$ J/s, and maintained the same elevation and point spacing even at high conversion ($X_A = 0.95$), to $8.4\times10^7$ J/s. The steady increase in Q indicates that as more reaction occurs

  

within a fixed reactor volume, the rate of energy release becomes denser as more ethylene and chlorine react to form ethylene dichloride. The steady point spacing throughout the graph signifies uniform heat distribution.

#### 4.1.8. Variation of Heat Generation per Unit Volume with Fractional Conversion

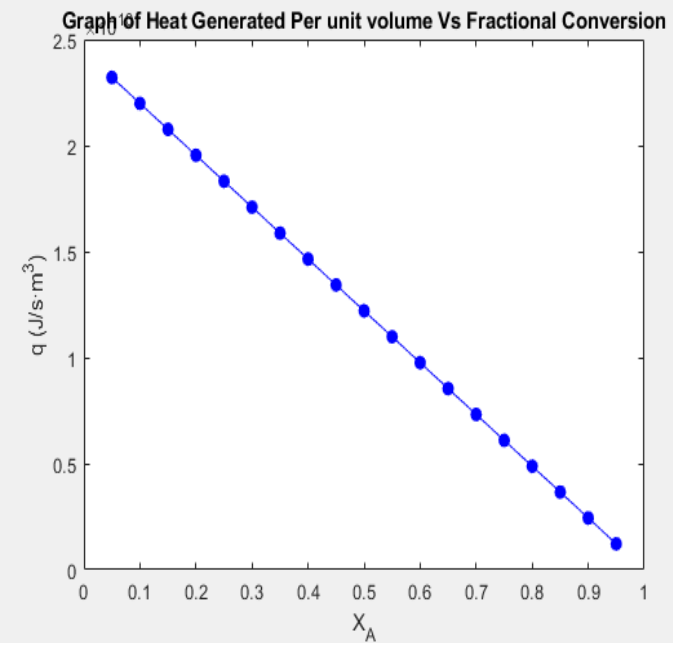


*Figure 10: Profile of Heat Generation per Unit Volume (q) with Fractional Conversion ($X_A$)*

The plot of heat generation per unit volume against conversion followed a regular exponential trend. At low conversion ($X_A$ = 0.05), q was about 2.3 × $10^{10}$ J/$m^3$·s, while at mid-range ($X_A$ = 0.5), it lowered to approximately 1.2 × $10^{10}$ J/$m^3$·s, and at high conversion ($X_A$ = 0.95), the value steadily dropped near 1.2 × $10^9$ J/$m^3$·s. The steady drop in q indicates that as more reaction occurs within a fixed reactor volume, the rate of energy release becomes denser. The consistent point spacing throughout the graph signifies uniform heat distribution at moderate conversion. This pattern highlights the importance of designing efficient cooling systems to dissipate localized heat loads within the reactor.

#### 4.1.9. Variation of Space Time with Reactor Volume

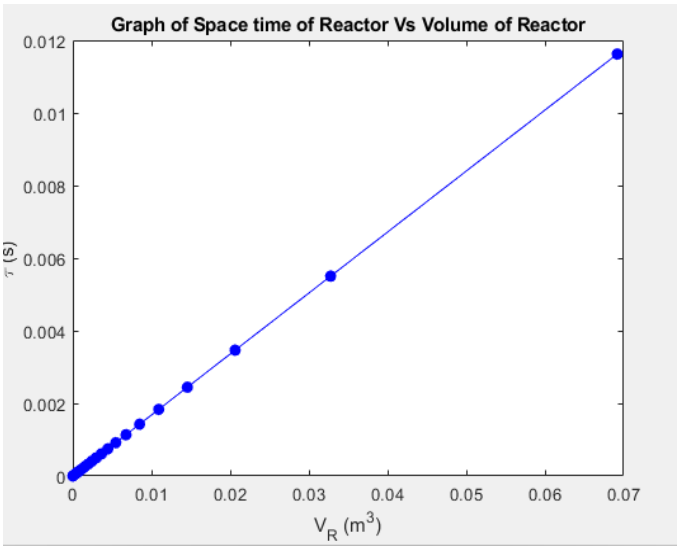


*Figure 11: Profile of Space Time (τ) with Reactor Volume ($V_R$)*

The graph showing the relationship between space time and reactor volume displays a smooth, upward, near-linear curve, indicating a direct proportionality between both variables. At a small reactor volume of approximately 0 $m^3$, the corresponding space time was about 3.2×$10^{-5}$ s, showing that the reactants spent very little time in the reactor. As the reactor volume increased to 0.003 $m^3$, the space time rose significantly to around 6.1×$10^{-4}$ s, while at a much larger volume of 0.069 $m^3$, the space time reached nearly 0.01 s. The even spread of data points across the plot signifies that as the reactor volume expands, the fluid spends more time in the reactor before leaving). The curve's mild slope at low volumes reflects efficient mixing and fast reaction rates, while its steepening toward higher volumes indicates slower kinetics and greater retention required to achieve higher conversions.

  

Journal of Engineering, Emerging Technologies and Applied Sciences
Volume: 03 Issue: 01 | March, 2026 Access point: https://www.ndu.edu.ng/jeetas

#### 4.1.10. Variation of Space Velocity with Reactor Volume

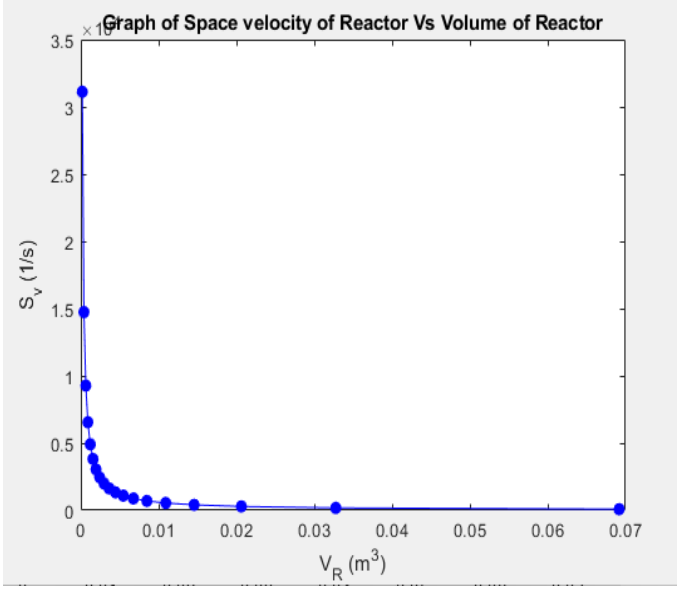


*Figure 12: Profile of Space Velocity ($S_V$) with Reactor Volume ($V_R$)*

The plot of space velocity against reactor volume exhibits a sharp inverse curve, confirming the reciprocal relationship between the two parameters. At a low reactor volume of about 0.00 $m^3$, the space velocity was very high, approximately 31,124 $s^{-1}$, indicating rapid feed turnover within the reactor. As the volume increased to about 0.00064$m^3$, the space velocity dropped significantly to roughly 9,280 $s^{-1}$, and further decreased to nearly 86 $s^{-1}$ at a larger volume of 0.069 $m^3$. The latter part of the curve becomes more flattened, showing that after a certain reactor size, further volume expansion has a smaller effect on space velocity reduction. Closely spaced points at low reactor volumes indicate fast flow and poor conversion potential, while the wider spacing at higher volumes reveals longer residence periods and improved reaction completion.

## 5. CONCLUSION

This work focused on the design of a Mixed Flow Reactor (MFR) for the production of ethylene dichloride (EDC) from the liquid-phase direct chlorination of ethylene. The modelling and simulation, carried out using MATLAB, provided insight into the influence of key operating and design parameters such as fractional conversion, reactor volume, temperature, space time, space velocity, and heat generation and the role of reaction kinetics in modelling and designing a model. Simulation results confirmed that chlorine is the limiting reactant, while ethylene is in excess, enabling a pseudo-first-order kinetic approach. Conversion was shown to improve with higher temperature, reactor volume, height, diameter, space time and quantity of heat generated but declined at space velocity and quantity of heat generated per unit volume of the reactor. The process was also confirmed to be strongly exothermic, with heat generation closely tied to conversion, underscoring the need for effective cooling. In summary, at an operating temperature of 357 K with appropriate reactor sizing ensures high conversion, efficient heat management, and safe, economical production of EDC. The following conclusions can be drawn;

i. The design and sizing parameters of reactor such as volume, height, diameter, space time, space velocity, quantity of heat generated and the quantity of heat generated per unit volume of the reactor at 95% fractional conversion were gotten as 0.069$m^3$, 0.7063m, 0.3532m, 0.01162seconds, 86.05seconds, 8.44 × $10^7$ J/s and 1.22× $10^9$ J/$sm^3$ respectively.
ii. The effect of fractional conversion on reactor parameters such as volume, height, diameter,

  

space time, space velocity, quantity of heat generated as well as the quantity of heat generated per unit volume of the reactor and the relationship between reactor parameters were simulated and presented in figure 3 to 12.

iii. Finally, based on the analysis of the results obtained and important knowledge gathered from literatures, the mixed flow reactor (MFR) is considered suitable for the Liquid phase direct chlorination of ethylene for ethylene dichloride production.

## REFERENCES

Abashar, M. (2004). Ethylene dichloride production in external-loop gaslift reactors. Journal of King Saud University - Engineering Sciences, 16(2), pp. 179–201.

Benvenuto, M. A. & Plaumann, H. (2021). Chapter 16, Ethylene dichloride. In Industrial Catalysis, De Gruyter eBooks, pp. 59–62.

Cherkasov, N., Adams, S. J., Bainbridge, E. G. A. & Thornton, J. A. M. (2022). Continuous stirred tank reactors in fine chemical synthesis for efficient mixing, solids-handling, and rapid scale-up. Reaction Chemistry & Engineering, 8(2), pp. 266–277.

Intratec. (2022). Ethylene Dichloride from Ethylene and Chlorine (LTC Process).

John, B. B. (2007). Reactor Design and Reactor Kinetics Engineering. 5 Edition,Butter-Worth-Heinemann.

Junsittiwate, R., Kodchakong, A. & Srinophakun, T. R. (2018). Ethylene Dichloride Production by Oxychlorination in a Fluidized Bed Reactor with CFD Model. Asian Journal of Applied Sciences, 6(5).

Kurta, S. A., Mykytyn, I. M., Khatsevich, O. M. & Ribun, V. S. (2018). Mechanism of catalytic additive chlorination of ethylene to 1,2-dichloroethane. Theoretical and Experimental Chemistry, 54(4), pp. 283–291.

Lakshmanan, A. & Biegler, L. T. (1997). A case study for reactor network synthesis: the vinyl chloride process. Computers & Chemical Engineering, 21, pp.785–790.

Montebelli, A., Tronconi, E., Orsenigo, C. & Ballarini, N. (2015). Kinetic and Modeling study of the ethylene oxychlorination to 1,2-Dichloroethane in Fluidized-BED reactors. Industrial & Engineering Chemistry Research, 54(39), pp. 9513–9524.

Moradi, Z. & Farsi, M. (2020). Simulation of direct chlorination of ethylene in a two-phase reactor by coupling equilibrium, kinetic and population balance models. Chemical Product and Process Modeling, 16(4), pp. 331–343.

Orejas, J. A. (2001). Model evaluation for an industrial process of direct chlorination of ethylene in a bubble-column reactor with external recirculation loop. Chemical Engineering Science, 56(2), pp. 513–522.

Process Insights, Inc. (2023). Safe operation of your EDC reactor. In ClearView Db Photometric Analyzer.

Saing, Z., Sudarto, M. A. & Faida, Z. (2020). A pre-designed study of the ethylene dichloride plant from ethylene and chlorine with 40,000 tons/year capacity. HAL (Le Centre Pour La Communication Scientifique Directe), 29(6), pp. 7145-7152.

Wachi, S. & Morikawa, H. (1986). Liquid-phase chlorination of ethylene and 1,2-dichloroethane. Journal of Chemical Engineering of Japan, 19(5), pp. 437–443.

Wang, M. & Ma, D. (2022). Reaction: direct chlorination of ethane to dichloroethane. Chem, 8(4), pp. 886–887.

Wosu, C.O. & Aworabhi, E. (2025a). Design Assessment of Flow Reactors for the Production of 1,000,000 tons per year of Ethyl Acetate from the Esterification Reaction of Acetic Acid and Ethyl Alcohol. UNIOSUN Journal of Engineering and Environmental Sciences, 7(1), pp. 14–24.

Wosu, C.O. & Aworabhi, E. (2025b). MFR Lifespan Improvement Using Standard Thickness Specification Models to Withstand the Effect of Temperature and Pressure During Cumene Production. International Journal of Engineering Inventions, 14(3), pp. 110–11.

  